Coherent resonance contributions in the reactions ^{6}Li$(d,\alpha)^{4}$He and ^{10}B$(d,p_0)^{11}$B at sub-Coulomb energies

G. Ruprecht,[1,*,†] K. Czerski,[1,2] D. Bemmerer,[1] M. Hoeft,[3] and P. Heide[1]
[1]*Technische Universität Berlin, IAPF, Sekr. PN 3-1, Hardenbergstrasse 36, 10623 Berlin, Germany*
[2]*Hahn-Meitner-Institut, Glienicker Strasse 100, 14109 Berlin, Germany*
[3]*International University Bremen, Campus Ring 12, 28759 Bremen, Germany*
(Received 1 January 2004; revised manuscript received 21 May 2004; published 30 August 2004)

The angular distribution of the reaction ^{6}Li$(d,\alpha)^{4}$He at deuteron energies below 100 keV and the total cross section as well as the angular distribution of the reaction ^{10}B$(d,p_0)^{11}$B at energies below 350 keV have been measured. Based on our experimental results and data of other authors, the reaction mechanism has been studied in a wide energy range, relevant for astrophysical applications. It has been found that in both cases broad resonances in the compound nuclei play the key role for the description of the excitation functions. The long-standing problems of describing the angular distributions could be solved for both reactions by assuming a coherent superposition between resonant and direct reaction amplitudes. A theoretical approach allowing for coherent calculations has been developed. Some astrophysical implications are discussed.

DOI: 10.1103/PhysRevC.70.025803 PACS number(s): 25.45.Hi, 24.30.Cz, 26.35.+c, 27.20.+n

I. INTRODUCTION

Nuclear reactions at projectile energies far below the Coulomb barrier are usually of astrophysical interest. However, because of the rapidly decreasing penetrability, the cross sections of nuclear reactions can experimentally be determined only down to a certain minimum projectile energy. Therefore, to obtain information about the nuclear rates in astrophysical plasmas, the experimental excitation curves have generally to be extrapolated towards lower energies. The situation gets even more complicated at energies low enough so that the electron screening effect, leading to an exponentiallike enhancement of the cross section, contributes significantly [1]. Thus, the extrapolation procedure can be carried out unambiguously only if the reaction mechanism is well known in a wide energy range. Here, we will study deuteron-induced reactions on ^{6}Li and ^{10}B nuclei which, on the one hand, are relevant for the primordial nucleosynthesis in inhomogeneous scenarios [2], but, on the other hand, are not yet understood as far as the reaction mechanisms are concerned.

In both reactions, the entrance channel threshold corresponds to a high excitation energy in the compound nuclei (22.3 MeV for ^{8}Be and 25.2 MeV for ^{12}C). This means that even at very low projectile energies many reaction channels are open and the level densities in the compound nuclei ^{8}Be and ^{12}C are relatively high. Therefore, microscopic reaction theories, such as the resonating group theory [3,4], generally being very successful in the description of low-energy nuclear reactions on light nuclei, cannot be applied here. Within those theories, any truncation of the number of reaction channels or of excited states leads inevitably to a not predicable, imaginary scattering potential and consequently to an uncertainty as well in the absolute value of the cross section as in the course of the excitation function. Here, we would like to present a theoretical approach based on the distorted wave Born approximation (DWBA) describing the direct part of the cross section and on a coherently added contribution of the relevant compound nucleus resonances. Because of the theoretical complications connected with the coherent superposition, in the past both contributions were usually added incoherently.

The importance of a coherent superposition of the direct and resonance contributions is particulary evident in deuteron-induced reactions on ^{6}Li. A few years ago we pointed out [5] that both the cross sections and the branching ratios of the mirror reactions ^{6}Li$(d,p_1)^{7}$Li and ^{6}Li$(d,n_1)^{7}$Be can be explained if an isospin-mixed resonance state, lying about 80 keV below the reaction threshold, is included. Due to the domination of the direct reaction amplitude, the resonance component could be added incoherently. The same resonance was found to contribute to the ^{6}Li$(d,\alpha)^{4}$He reaction [6]. However, under the assumption of incoherent superposition of the reaction amplitudes, the angular distribution of this reaction could be described only by changing the sign of the imaginary part of the optical potential in the initial channel. It was pointed out in Ref. [7] that the coherent addition of the resonance amplitude can remove this ambiguity. In the present work, supported by some experimental data, detailed calculations of the cross section and angular distribution for the reaction ^{6}Li$(d,\alpha)^{4}$He performed within our approach, will be given, and consequences for the determination of the electron screening energy and the astrophysical S factor will be discussed.

The theoretical description of the angular distribution and the absolute cross section of the ^{10}B$(d,p)^{11}$B reaction provides another long-standing problem. Already in 1973 it was realized [8] that the angular distribution for the transitions to the different final states of ^{11}B cannot be described in the framework of the standard DWBA theory for a wide deuteron energy range. Additional contributions to the reaction

*Electronic address: ruprecht@physik.TU-Berlin.DE
†Present address: TRIUMF, 4004 Wesbrook Mall, Vancouver, B.C., V6T 2A3, Canada

amplitude, due to exchange terms and finite range corrections, were proposed. Furthermore, the absolute cross sections measured by different groups differ from each other by a factor of 100. The low-energy measurements and the theoretical calculations performed recently [9] do not change this situation considerably. The correction to the optical potential in the initial channel, supposed to include the antisymmetrization effects, could properly describe the measured angular distribution for the ground-state transition. However, the presented experimental differential cross section differs substantially from those measured by other authors and from our experimental data achieved in the similar energy region [10]. In this paper, all measurements of the $^{10}\mathrm{B}(d,p)^{11}\mathrm{B}$ reaction performed since 1954 for deuteron energies below 3 MeV will be compared. It will be shown that the resulting excitation curve as well as the angular distribution can be explained if the standard DWBA contribution will be completed by a coherent superposition of the excitation of the giant dipole resonance (GDR) and a giant quadrupole resonance (GQR) as doorway states in the compound nucleus $^{12}\mathrm{C}$.

Before we present the results of our calculations for the deuteron-induced reactions on $^{6}\mathrm{Li}$ and $^{10}\mathrm{B}$, some details of the theoretical approach will be given in the next section.

II. THEORETICAL ASPECTS

The direct contribution to a nuclear reaction has been calculated within the DWBA model with the zero range approximation. Considering the accuracy of the experimental data, this approximation is sufficient. Computer codes for DWBA usually give the results as reduced cross sections for each angular momentum transfer which is allowed by selection rules. However, for a coherent superposition, we need the transition (T) matrix with the correct phase. Additionally, direct and resonance T matrices must be given in the same representation.

The resonance T matrix T^R is parametrized by the total angular momentum J of the compound level, the orbital angular momenta L_α, L_β and the spins S_α, S_β of the entrance (α) and exit (β) channel, respectively. The energy dependence (here for $\alpha \neq \beta$) is given by the Breit-Wigner formula (see, e.g., [11])

$$T^R = -2e^{i(\xi_\alpha+\xi_\beta)}\sqrt{\rho_\alpha\rho_\beta P_\alpha P_\beta}\frac{\gamma_\alpha\gamma_\beta}{\Gamma/2 + i(E_R - E)}, \qquad (1)$$

where $\gamma_\alpha\gamma_\beta$ is the product of the reduced level width amplitudes, E_R is the resonance energy, and Γ is the total width. These are the free parameters in this model. The penetrations P are defined as $1/[F_L^2(\rho)+G_L^2(\rho)]$, where F and G are the regular and irregular Coulomb functions dependent on $\rho = kr$, where k denotes the wave number and r is the distance between the reacting nuclei in the corresponding channel. The scattering phases ξ are defined as $\xi = \sigma_L(\rho) - \phi_L(\rho)$, with the Coulomb phase $\sigma_L(\rho) = \arg\Gamma(1+L+i\eta)$ and the hardcore phase $\phi_L(\rho) = \arg(G+iF)$. η is the Sommerfeld parameter. The penetration factors as well as the scattering phases have to be calculated at the nuclear radius of the entrance and exit channel, respectively. For definitions of the Gamma function $\Gamma()$ and the Coulomb function, see [12]. The corresponding cross section yields the well-known Lorentz formula.

On the contrary, the T matrix for the direct contribution is usually calculated by means of *transfer* variables: orbital angular momentum transfer l, spin transfer s, total angular momentum transfer j. Computer codes for DWBA calculate reduced T matrices depending on the transfer variables l, s, and j. For a coherent superposition, DWBA T-matrix elements must be reordered from $\{lsj\}$ to $\{JLS\}$ representation. Unfortunately, phases are not uniformly defined by different authors, so the T matrix definitions have to be used carefully. After the reordering process the resonance matrix elements have to be added. Finally, LSJ matrices must be transformed to unpolarized differential cross sections via the well-known relation found by Blatt and Biedenharn [13] (see also [14]):

$$B_K = \frac{1}{4k_\alpha^2}\frac{1}{\hat{I}_a^2\hat{I}_A^2}\sum_{S_\alpha S_\beta}(-)^{S_\beta - S_\alpha}\sum_{JL_\alpha L_\beta \overline{JL}_\alpha \overline{L}_\beta}\tilde{Z}(L_\alpha J\overline{L}_\alpha\overline{J},S_\alpha K) \times \tilde{Z}(L_\beta J\overline{L}_\beta\overline{J},S_\beta K)\tilde{T}^{J*}_{\beta L_\beta S_\beta,\alpha L_\alpha S_\alpha}\tilde{T}^{J}_{\beta\overline{L}_\beta S_\beta,\alpha\overline{L}_\alpha S_\alpha}, \qquad (2)$$

where

$$\tilde{Z}(L_\lambda J\overline{L}_\lambda\overline{J},S_\lambda K) = \hat{L}_\lambda\hat{\overline{L}}_\lambda\hat{J}\begin{pmatrix} L_\lambda & \overline{L}_\lambda & K \\ 0 & 0 & 0\end{pmatrix}W(L_\lambda J\overline{L}_\lambda\overline{J},S_\lambda K),$$

$$\text{with } \hat{L}_\lambda = \sqrt{2L_\lambda+1},\ \lambda = \alpha,\beta.$$

I_a and I_A are the spins of the projectile and the target nucleus. The round bracket denotes the Clebsch-Gordan coefficient, here for the coupling $\mathbf{L}_\alpha + \overline{\mathbf{L}}_\alpha = \mathbf{K}$, and W is the Wigner coefficent. B_K are Legendre polynomial coefficients of the differential cross section

$$\frac{d\sigma}{d\Omega} = \sum_K B_K P_K(\cos\theta), \qquad (3)$$

at the reaction angle θ in the c.m. system. We define the anisotropy coefficients

$$A_K = B_K/B_0. \qquad (4)$$

All results presented here are expressed by these coefficients and the total cross section $\sigma(E)$, represented by means of the S factor, defined by

$$S(E) = \sigma(E)E\exp\sqrt{\frac{E_G}{E}}. \qquad (5)$$

The Gamow energy E_G amounts to 13.3 MeV for $^{6}\mathrm{Li}+d$ and 41.0 MeV for $^{10}\mathrm{B}+d$. To consider the electron screening, the S factor must be multiplied by the screening enhancement factor $f(E)$. For projectile energies much larger than the screening energy U, a good approximation is given by (see [1])

$$f(E) = \frac{\sigma(E+U)}{\sigma(E)} \approx \exp\left(\frac{1}{2}\sqrt{\frac{E_G}{E}}\frac{U}{E}\right). \qquad (6)$$

For numerical calculations the computer application Di-Wan has been developed. The code for the direct contribu-

tion is taken from DWUCK4, written by Kunz [15,16]. His program, written in Fortran, is able to calculate reduced cross sections in DWBA zero range approximation with projectile and ejectile being in any combination of spin 0, 1/2, and 1. The code was integrated into DiWan and extended by the resonance contribution after transformation from the $\{lsj\}$ to the $\{LSJ\}$ representation as described above. DiWan calculates for a given energy range cross sections and S factors as well as Legendre coefficients of the angular distribution. Both direct and resonance contribution can optionally be combined coherently or incoherently. The resonance parameters, as given in Eq. (1), and the strength of the direct contribution, expressed by the zero range parameter D_0^2, can be varied. The resulting excitation curves can be directly compared with experimental data. Further details can be found in [17].

In the following sections we discuss the experimental data, partially completed by our own measurements, and theoretical results for the two reactions.

III. THE ^{6}Li$(d,\alpha)^4$He REACTION

As mentioned in the introduction, the ^{6}Li$(d,\alpha)^4$He reaction at low deuteron energies is dominated by a broad resonance [6]. The energy position E_R corresponding to an excitation energy of $E_x \approx 22.2$ MeV in the ^{8}Be compound system lies about 80 keV below the reaction threshold. The total width Γ is about 800 keV (see [18]) and the quantum numbers are $J^\pi = 2^+$. Because of the identical particles in the exit channel, only even anisotropy coefficients appear. In the following we only regard the A_2 coefficient.

Accurate data exist both for the total cross sections and for the angular distributions down to 15 keV [19–21]. Surprisingly, around $E_{\text{c.m.}} = 100$ keV the anistropy coefficient A_2 seems to change sign. To confirm and improve the accuracy of the data, we performed our own measurements in this energy region, using the following setup.

A. Experimental setup

Deuteron ions are generated in the high-frequency ion source of the 200 kV electrostatic Cockroft-Walton accelerator. After extraction and acceleration, the ions are focused by an electric quadrupole pair. The following analyzing magnet selects the D^+ beam component, which enters the target chamber after a distance of 3 m in a vacuum of 10^{-4} Pa. Inside the chamber (see Fig. 1) two slits reduce the beam diameter to 5 mm. In early measurements (1998) thick targets (100 μg/cm^2 ^{6}LiF) were used. In a refined measurement (2000) the targets were composed of a 10 μg/cm^2 ^{6}LiF layer on a 0.2 mm copper backing. By means of a copper plate with a 3 mm hole on the front side a clearly defined beam spot could be achieved. The 11 MeV alpha particles were background free detected by 100 mm^2 Canberra PIPS detectors (for energy spectra see [6,17]). With a distance of 12 cm from the target to the detectors, the solid angle precision was better than 5%. To reject elastically scattered deuterons the detectors were covered by aluminum foils. Due to the 90° symmetry of the angular distribution of the identical α particles, measurements only at backward angles are sufficient. For current measurements and suppression of secondary electrons, the target system was surrounded by a cylinder with openings for the incoming beam and the ejectiles.

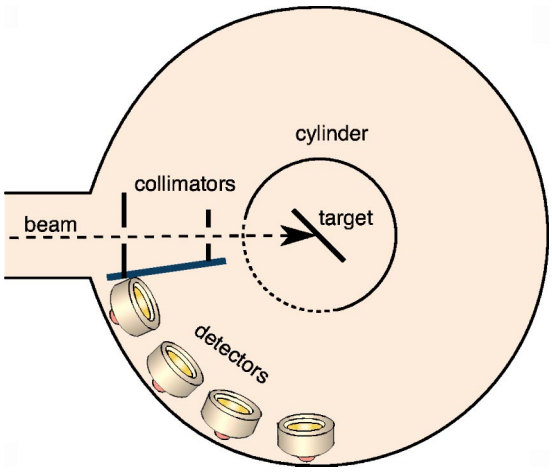

FIG. 1. (Color online) The target chamber used for the $d+^6$Li reaction.

Data were collected with a VERSAmodule Eurocard (VME) system and could be evaluated online. So the state of the target could be directly observed and changes of the target surface (e.g., the buildup of a carbon layer or sputtering) could be noticed immediately by observing a decrease of the yield.

B. Results and calculations

Our experimentally determined anisotropy coefficients for the ^{6}Li$(d,\alpha)^4$He reaction are presented in Table I and, together with measurements from Refs. [19–21], depicted in Fig. 2. Obviously, A_2 increases with increasing energy. Around 50 keV A_2 tends to be negative ($A_2 \approx -0.05$). This anormal behavior was originally observed by Refs. [20,21] and was confirmed by our measurements with improved precision.

For the calculation of the direct contribution the zero range parameter D_0^2 for the $d \otimes d = \alpha$ cluster is needed. The

TABLE I. A_2 coefficients for the ^{6}Li$(d,\alpha)^4$He reaction. $E_{\text{c.m.}}^{\text{eff}}$ is the effective energy in the c.m. system.

$E_{\text{c.m.}}^{\text{eff}}$ [keV]	A_2	ΔA_2	Target
21.89	0.1	0.1	10 μg/cm^2, 2000
25.60	−0.03	0.03	10 μg/cm^2, 2000
29.31	−0.005	0.025	10 μg/cm^2, 2000
33.02	0.020	0.025	10 μg/cm^2, 2000
36.73	0.033	0.008	10 μg/cm^2, 2000
41.15	−0.015	0.015	100 μg/cm^2, 1998
58.96	−0.045	0.010	100 μg/cm^2, 1998
73.21	−0.057	0.008	100 μg/cm^2, 1998
78.70	−0.040	0.010	100 μg/cm^2, 1998
80.41	0.00	0.03	100 μg/cm^2, 1998

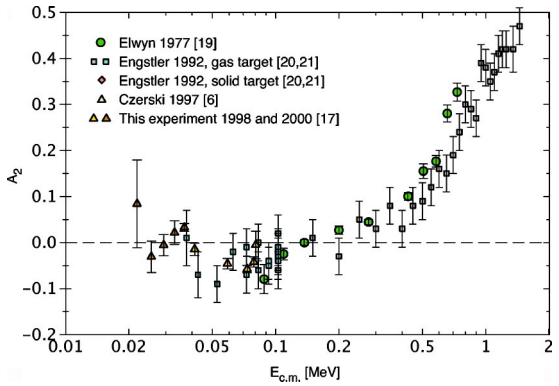

FIG. 2. (Color online) Measured A_2 coefficient for the ^{6}Li$(d,\alpha)^4$He reaction in dependence on the deuteron energy in the c.m. system (logarithmic scale).

D_0^2 values used by different authors vary between 1 and 1000×10^4 MeV^2 fm^3, so we decided to use it as a free fit parameter determining the overall strength of the direct contribution. Additionally, the optical potentials are needed for the reaction channels and the bound state. They are listed in Table II together with potentials used for the $d+^{10}$B reaction (see Sec. IV B). All potentials have the simple Saxon-Woods shape

$$V(r) = V_R f(x_R) + iV_I g(x_I),$$

$$\text{where } g(x_n) = \frac{df(x_n)}{dx_n},\quad f(x_n) = \frac{1}{1+e^{x_n}},$$

$$\text{and } x_n = \frac{r - r_n A^{1/3}}{a_n}. \tag{7}$$

The parameters are as defined by Ref. [15]. The potential given by Ref. [22] results from deuteron scattering on ^{12}C, but can be well applied for other light nuclei. The influence of spin-orbit terms has been tested to be negligible. The spectroscopic factors of the deuteron within the ^{6}Li nucleus were taken from Ref. [25].

Theoretically, a resonance state of a compound nucleus is determined by the reduced width amplitudes for all channels, orbital momenta L and total spins S. Assuming that mainly the s wave contributes to the entrance channel $d+^6$Li, then only the combination $\{L_\alpha,S_\alpha\}=\{0,2\}$ is possible to reach the 2^+ resonance state. For the exit channel $\alpha+\alpha$ only $\{L_\beta,S_\beta\}=\{2,0\}$ is possible. Altogether, the parameters used to fit the

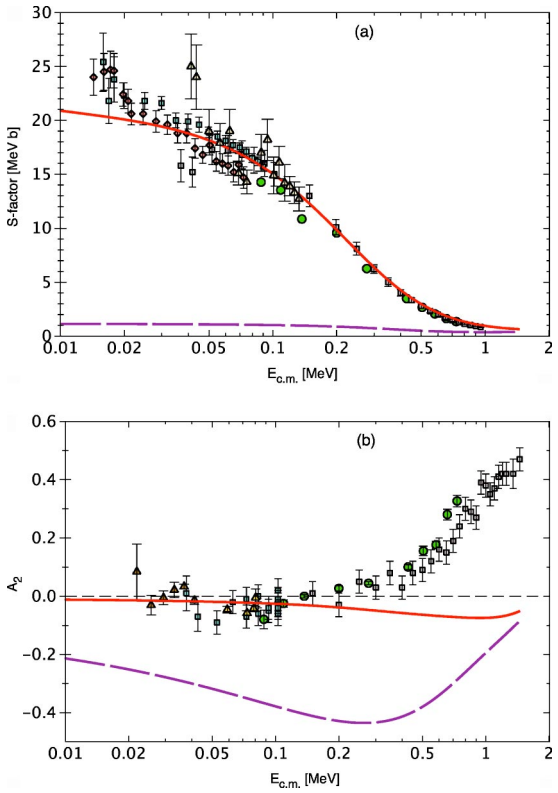

FIG. 3. (Color online) Energy dependence of the calculated and measured S factor (a) and anisotropy coefficient (b) for *incoherent* "superposition" ($D_0^2=22\times10^4$ MeV^2 fm^3). The dashed line shows the direct contribution only. The symbols used are the same as in Fig. 2.

experimantal data are the total resonance width Γ, the resonance energy E_R, the product of the reduced width amplitudes $\gamma_\alpha\gamma_\beta$ and the zero range parameter D_0^2.

Figure 3 shows the results obtained for an incoherent addition of the direct and resonance contributions. While the astrophysical S factor fits the data points very well, the anisotropy coefficient A_2 doesn't bear any resemblance to the measurements. Obviously, the incoherent method is not applicable to describe the angular distribution.

In Fig. 4 the same data are shown together with a *coherent* superposition of the reaction amplitudes. The resonance parameters and D_0^2 have been adjusted visually to best fit the experimental S factor and angular distribution simultaneously—an automatic fit procedure is not yet provided by the code. Because of a relatively large resonance

TABLE II. Optical potentials used for the ^{6}Li$(d,\alpha)^4$He and ^{10}B$(d,p)^{11}$B calculations. E is the energy in the c.m. system. The depths for the bound states $d+^4$He and $n+^{10}$B are only used as starting values for the program. Their imaginary parts are not used.

Potential	Ref.	V_R/MeV	r_R/fm	a_R/MeV	V_I/MeV	r_I/fm	a_I/fm
$d+^6$Li, ^{4}He, or ^{10}B	[22]	−115	0.9	0.9	$26+1.32E$	$2.48-0.0036E$	0.45
$\alpha+^4$He	[23]	−117	1.14	0.6	−1	1.14	0.6
$p+^{11}$B	[24]	$-63.4+0.3E$	$1.15-0.001E$	0.57	$3.64+2.56E$	$=R_R$	0.5
$n+^{10}$B	[24]	$-60+0.3E$	″	″	$2.56E$	″	″

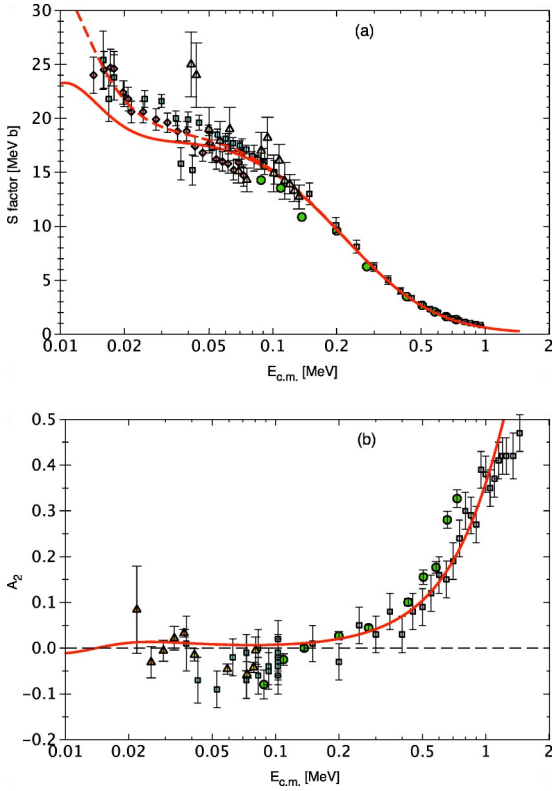

FIG. 4. (Color online) Energy dependence of the calculated and measured S factor (a) and anisotropy coefficient (b) for *coherent* superposition. The dashed curve in (a) corresponds to a screening potential of $U=190$ eV. The symbols used are the same as in Fig. 2.

width, it was possible to fit both reaction contributions for deuteron energies larger than 50 keV, where the enhancement of the cross section due to the screening effect can be neglected. The adjusted values of parameters are as follows: $D_0^2=1.0\times10^4$ MeV^2 fm^3, $E_R=-0.08$ MeV, $\Gamma=0.56$ MeV, $\gamma_\alpha\gamma_\beta=-0.133$ MeV, $U=190$ eV. The zero range parameter is of the same order of magnitude as that used for (d,p) reactions $(1.55\times10^4$ MeV^2 fm$^3)$.

C. Discussion

Both coherent and incoherent S factor calculations fit the measured data very well. Only at very low energies (notice the logarithmic scale) the curves differ from each other and from the experimental data. The enhancement of the experimental S factors can be explained by the electron screening effect. According to Eq. (6) we can determine, for the coherent calculation, the S factor at zero deuteron energy $S(0)=23\pm2.5$ MeV b and the screening energy $U=190\pm50$ eV. The small absolute error of $S(0)$ mainly arises from the precise measurement of Elwyn *et al.* [19]. The value of the screening energy is in agreement with the upper limit of the adiabatic estimation 186 eV. The larger U values of 380 ± 250 eV for solid targets and 330 ± 120 eV for gaseous targets, and consequently the lower value of $S(0)=16\pm3$ MeV b, published by Engstler *et al.* [20,21], rely on an extrapolation by a polynomial fit only. Similar large screening energies (320 ± 50) have recently been obtained using the Trojan Horse method [26,27]. Obviously, our lower screening energy is due to the influence of the subthreshold resonance, which is not taken into account by Refs. [20,21]. The high screening values obtained by Refs. [26,27] are based mainly on two S factor values at the lowest energies which seem to be systematically underestimated compared to Refs. [20,21] and our own measurements [6].

Concerning the A_2 curve, the measured data are now in very good agreement with the coherent superposition calculations. This is a remarkable result because the interference effect can hardly be seen in the total cross section or S factor, but rather in the angular distribution. Although a variation of the fit parameters can produce a negative A_2 (see [7]) in the region 50–100 keV, the curve shown here has only nearly zero values in this region. We decided for the latter choice of parameters because the overall S factor as well as A_2 data are fitted best by this set.

TABLE III. Experimental data sets for the ^{10}B(d,p_0) reaction and the applied renormalization factors

Reference	$E_{c.m.}$ Range [MeV]	Absolute Uncertainty	Renormalization Factor
Burke 1954 [28]	0.59–1.53	30%	0.12
Paris 1954 [29]	0.13–0.57	10%	1
Marion 1956 [30]	0.74–2.51	15%	3.13
Arena 1972 [34]	0.58–2.08	10%	3.81
Arena 1977 [35]	0.83–1.67	10%	4.05
Yan 1997 [9]	0.07–0.14	10%	1
This work 2001 [10,38]	0.10–0.28	10%	1

IV. THE ^{10}B$(d,p_0)^{11}$B REACTION

The Q value for this reaction is 9.23 MeV. The separation energy of 25.19 MeV for the $d+^{10}$B system corresponds to an excitation energy in ^{12}C where the level density is relatively high. It is also the region where giant resonances are expected. Before theoretical calculations were performed the reevaluation of existing experimental data was a major task as explained in the following section.

A. Experimental data

A lot of experimental data for $d+^{10}$B reactions exists for energies down to $E_{lab}=36$ keV [9,28–37]. While the angular distributions measured by different authors are mostly in good agreement, there exists a problem of absolute values of the cross section, varying by a factor up to 30 (see Table III). The authors have no explanations for these deviations. Nevertheless, excitation curves obtained from different authors have similar shapes in overlapping energy regions. Therefore, we consider it justified to renormalize the data sets, so that the absolute values are similar in the overlapping regions. As reference set we decided for the data of Paris [29], because they were in best agreement with the other measurements.

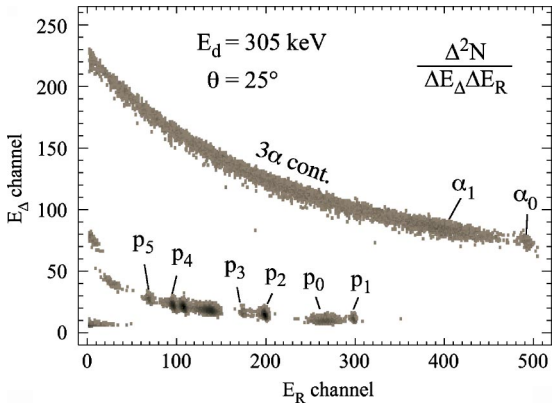

FIG. 5. Particle telescope spectrum for the $^{10}B+d$ reactions.

Some data sets were presented by authors as differential cross sections for three or four angles at many projectile energies [28,30,34]. Other authors measured a precise angular distribution for only a few energies [28–31,33,35]. Sometimes the measured data were presented more complicated (see [29]) or were normalized to other data. Therefore, we had to carry out a reevaluation of every data set to obtain S factors and anistropy coefficients. The S factors deduced from the experimental data presented here had to be renormalized. The renormalization factors are listed in Table III.

As can be seen in Fig. 6, the S factor data give a relatively consistent picture. There is an overall increase of the S factor with decreasing energy and a broad resonance at $E_{\mathrm{c.m.}}=1.4$ MeV. Additionally, a double resonance structure at $E_{\mathrm{lab}}\approx 500$ keV is visible. A similar resonance structure in the corresponding excitation energy region was also found in the photoreactions $^{12}\mathrm{C}(\gamma,p)^{11}\mathrm{B}$ and $^{12}\mathrm{C}(\gamma,n)^{11}\mathrm{C}$ [40].

At low energies relevant for astrophysical applications, the absolute S factors and angular distribution have been recently measured by Yan *et al.* [9]. Whereas the S factor values agree with those of Paris very well, the anisotropy coefficient of the angular distribution A_1 has the opposite sign compared to the results of Paris.

In our experiment, we measured angular distributions and the astrophysical S factors at the c.m. energies between 100 and 300 keV, which enabled us to check the overall normalization of the absolute cross section and clarify the deviations in the angular distribution. As previously described [10,38], the experiment was performed with the 360 kV electrostatic accelerator at the Technical University Berlin. In order to resolve different proton and alpha exit channels, we used a particle-telescope system consisting of a thin ΔE detector of 15 μm thickness and a total energy E detector with a thickness of 500 μm and an active area of 50 mm^2. A typical dual-parameter energy spectrum is presented in Fig. 5. Since the range of protons from the ground-state transition was larger than the thickness of the E detector, the corresponding spectral line is characteristically broadened and shifted towards lower energies. The distance between the detector and the target amounted to 52 ± 2 mm.

Angular distribution measurements were carried out at 15 different angles between 15° and 130° with a thin ^{10}B target (30 μg/cm^2) on Al backing (30 μg/cm^2); both layers were enclosed by a thin carbon foil (10 μg/cm^2). The $^{10}\mathrm{B}(d,3\alpha)$ reaction, being isotropic in the center-of-mass system (c.m.s.), was used for a solid angle calibration at all scattering angles. The resulting anisotropy coefficients for the $^{10}\mathrm{B}(d,p_0)^{11}\mathrm{B}$ reaction at the c.m. energies 137 and 254 keV are in good agreement with data from Paris but disagree with results of Yan *et al.* [9] (see Fig. 7). Contrary to us, Yan *et al.* used silicon surface barrier detectors and thick targets, limiting the minimum scattering angle to 60°.

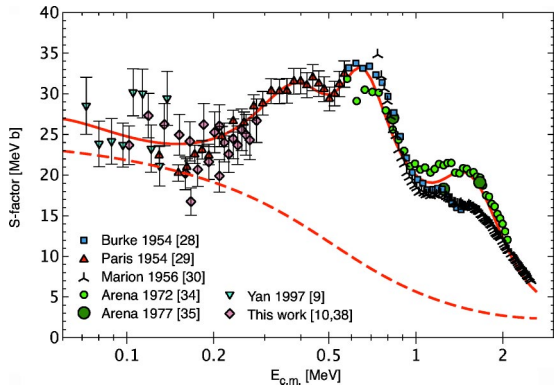

FIG. 6. (Color online) S factor for the $^{10}\mathrm{B}(d,p_0)^{11}\mathrm{B}$ reaction. The dashed line shows the direct contribution only.

The absolute cross sections were determined using a thick boron target (100 μg/cm^2) on a Ta backing and measuring the thick-target yield at the single backward angle of 135°. The thick-target yield was corrected for the observed angular

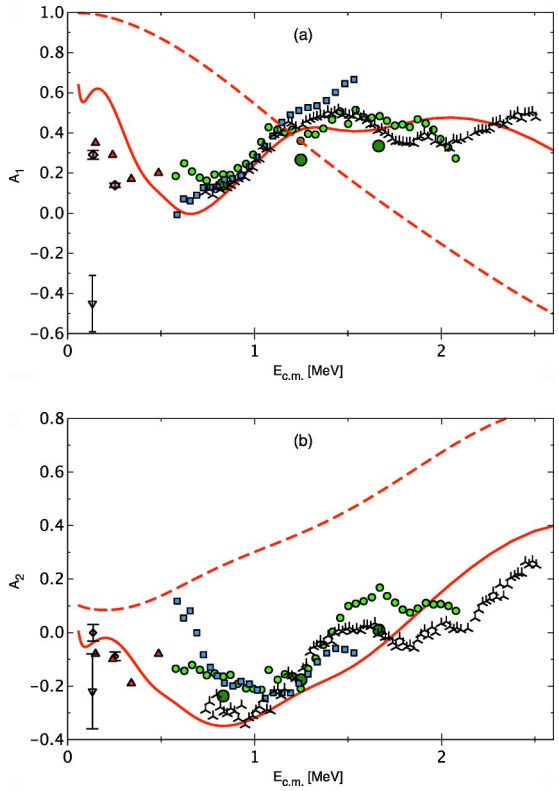

FIG. 7. (Color online) Anisotropy coefficients A_1 (a) and A_2 (b) for the $^{10}\mathrm{B}(d,p_0)^{11}\mathrm{B}$ reaction. The dashed line shows the direct contribution only. The symbols used are the same as in Fig. 6. For reasons of clarity, error bars $<10\%$ are omitted.

distribution and for the oxygen contamination of the target, determined by energy-dispersive x-ray microspectroscopy (EDX). The effective projectile energy within the target was evaluated taking into account a strong energy dependence of the cross section [38,39]. The resulting S factors are in good agreement with other low-energy measurements from Yan *et al.* and Paris. The deviations in the angular distribution determined by Yan *et al.* do not affect their S factor values because the yield measurements were performed at 90° where the differential yield approximately reaches its mean value.

B. Calculations

As far as is known, quantum numbers of the resonances relevant for this energy region are $J^\pi = 1^-$ (see [18]) and isospin $T=1$. They can be regarded as part of a fragmented GDR of the ^{12}C nucleus as shown in the results obtained for photoreactions [40]. In that work, also an isospin $T=0$ admixture of 10% was determined, which allows for excitation of the GDR in the initial channel $d+^{10}$B. The orbital angular momentum of the initial channel is restricted to 1 or 3, while the spins (1^+ and 3^+, respectively) couple to a minimum of 2. In the exit channel more combinations are possible. We decided for the values with the lowest L, $\{L_\beta, S_\beta\}=\{0,1\}$, which shows the strongest interference effect in the A_2 coefficient; calculations with other quantum numbers yield no better results. However, the energy dependence of the A_1 coefficient could not be described well by only the GDR contribution. It was necessary to include a small 2^+ resonance contribution to obtain the final results shown in Figs. 6 and 7. This contribution can be considered as part of a giant quadrupole resonance. Investigations of inelastic proton scattering on ^{12}C [41] pointed to a large quadrupole strength as a doorway state in the energy region of interest. For the two low-lying resonances we suppose that they have similar total and reduced partial widths (see Sec. IV C).

The description of the experimental data for the S factor as well as for the angular distribution shown in Figs. 6 and 7 could be obtained simultaneously including the following resonances:

(i) Two narrow 1^- resonances at $E_R=0.380$ and 0.610 MeV with $\gamma_\alpha\gamma_\beta=0.15$ and 0.14 MeV, respectively, and a total width of $\Gamma=0.366$ MeV

(ii) A broad 1^- resonance at $E_R=1.61$ MeV, $\gamma_\alpha\gamma_\beta=-0.567$ MeV and $\Gamma=1.24$ MeV.

(iii) A broad 2^+ resonance at $E_R=1.355$ MeV, $\gamma_\alpha\gamma_\beta=0.0642$ MeV and $\Gamma=0.710$ MeV.

The zero range parameter was fixed to the usual value for (d,p) reactions, i.e., $D_0^2=1.55\times10^4$ MeV fm^3 and the spectroscopic factor was taken from Ref. [42]. The optical potentials for the proton and neutron are derived from Watson [24] and were used unchanged as given in Table II and Eq. (7). The resulting curves are shown in Figs. 6 and 7, together with a calculation performed without any resonances.

C. Discussion

The S factor data measured by different authors and differing by a factor of up to 30, give a consistent curve when normalized to Paris [29], which is in very good agreement with the low-energy results of Yan *et al.* [9] and of the present work. The experimental angular distributions, expressed by A_1 and A_2, also appear to be consistent for energies up to 3 MeV. The strength of the fitted direct reaction contribution provides an additional argument for the reliability of the absolute S factors and the applicability of our theoretical model. In fact, no change of the standard value of the zero range parameter D_0^2 was necessary. Consequently, we can estimate the value of the S factor at the deuteron energy zero, being important for astrophysical applications, to about $S(0)=27\pm3$ MeV b.

The excitation function of the ^{10}B$(d,p_0)^{11}$B reaction is clearly dominated by three 1^- resonances. Since their positions, widths, and relative strengths correspond to those observed in photoreactions [40] on ^{12}C, they can be interpreted as part of the fragmented GDR in the compound nucleus ^{12}C. The experimental S factor values could also be described with an incoherent calculation, but the simultaneous description of $A_1(E)$ as well as $A_2(E)$ failed. As can be seen in Fig. 7, the direct contribution cannot explain the angular distribution. An incoherent calculation even increases the deviation from the experimental data. A coherent superposition of the three 1^- resonances mentioned above yields a $S(E)$ and $A_2(E)$ curve qualitatively reproducing the experimental data. However, the $A_1(E)$ curve can only be explained with a small contribution of the 2^+ resonance, which also has been observed by Ref. [41] and interpreted as a being part of a GQR.

As stated before, the excitation of the GDR in the $d+^{10}$B system is only possible due to an isospin impurity which can be caused by an internal isospin mixing. The electromagnetic interaction leads to a mixing of closely lying states of a similar internal structure having the same spin and parity but differing in isospin by one unit. This effect can be caused by two resonances: one with a large proton and a small neutron width and the other with a n/p branching ratio turned around (see [5]). Indeed, the "twin" resonances at 0.38 and 0.61 MeV have the same quantum numbers and nearly the same energy. Also the proton-to-neutron ratio fluctuation has been observed in photoreactions [40]. Additionally, a strong suppression of the ^{10}B$(d,p_2)^{11}$B/^{10}B$(d,n_2)^{11}$C ratio on the low-energy side of the resonances has been measured by Ref. [43]. Finally, in contradiction to Ref. [9], the theoretical model presented here favors the positive value of the A_1 coefficient for very low energies (see also end of Sec. IV A and Fig. 7).

V. CONCLUSIONS

The calculations presented here show that interference between compound nucleus and direct reaction amplitudes can have a strong effect on the cross sections and angular distributions, while an incoherent calculation cannot explain the measured data. The higher effort that is necessary in the calculations due to the different angular momentum presentation of both models is recompensed by good fits of the experimental data, simultaneously for the S factor as well as for the angular distribution over a wide energy range. No change

of the standard optical potentials is necessary and the standard DWBA method is fully sufficient.

Applying this method to the $^{6}\mathrm{Li}(d,\alpha)^{4}\mathrm{He}$ and $^{10}\mathrm{B}(d,p_0)^{11}\mathrm{B}$ reactions, some physical effects become visible. For the $^{6}\mathrm{Li}(d,\alpha)^{4}\mathrm{He}$ reaction one single, subthreshold 2^+ resonance is appropriate to describe all experimental data and a screening value of 190 ± 50 eV can be derived. An interesting point here is the strong interference at high energies dominating the angular distribution far outside the resonance range. For the $^{10}\mathrm{B}(d,p_0)^{11}\mathrm{B}$ reaction an aspect dealt here concerns long-standing differences of the total cross section as well as the angular distribution investigated by different groups in the last 50 years. After the reevaluation and renormalization of high-energy data, one obtains a consistent *S* factor curve, being also in agreement with low-energy values of Yan *et al.* [9] and of the present work. We argue that the strong resonance structures visible in the *S* factor are part of the fragmented giant dipole resonance, observed previously in the photoreactions on ^{12}C [40]. The excitation of the giant dipole resonance in the deuteron-induced reaction on ^{10}B is possible only due to its significant isospin impurity [40]. Consequently, two resonances lying at c.m. energies of 0.38 and 0.61 MeV can be interpreted as a doublet of isospin mixed states. The experimental angular distribution could be fitted very well by applying a coherent superposition of direct and resonance amplitudes, whereby a small contribution of the giant quadrupole resonance at the c.m. energy of 1.36 MeV was additionally needed to describe the A_1 anisotropy coefficient.

In general, due to the low amount of deuterons (10^{-4} of the amount of protons) in the standard homogeneous Big Bang nucleosonthesis (BBN) model, deuteron-induced reactions do not play an important role in astrophysical network calculations. However, as shown in [38], the $^{10}\mathrm{B}(d,n)^{11}\mathrm{C}$ reaction contributes to the ^{11}B production via the β^+ decay of ^{11}C after the BBN. For a baryon-to-photon ratio of $\eta=2\times10^{-10}$ it can contribute $\approx$10% to the ^{11}B production. The $^{10}\mathrm{B}(d,n)^{11}\mathrm{C}$ reaction rate can be estimated by the mirror reaction $^{10}\mathrm{B}(d,p_0)^{11}\mathrm{B}$ investigated here. A more precise analysis has to consider the mentioned isospin mixture, which will be a future task.

Finally, the results of an analysis of the cosmic microwave background radiation [44] predict a baryon-to-photon ratio being slightly larger than the ratio obtained within the standard BBN model [45]. Therefore, the inhomogeneous nucleosynthesis models for which deuteron-induced reactions have a much larger impact still remain important.

[1] H. J. Assenbaum, K. Langanke, and C. Rolfs, Z. Phys. A **327**, 461 (1987).
[2] R. A. Malaney and G. J. Mathews, Phys. Rep. **229**, 145 (1993).
[3] D. Baye and P. Descouvement, J. Phys. Soc. Jpn. **58**, 103 (1989).
[4] K. Langanke, Adv. Nucl. Phys. **21**, 85 (1994).
[5] K. Czerski, H. Bucka, P. Heide, and T. Makubire, Phys. Lett. B **307**, 20 (1993).
[6] K. Czerski, A. Huke, H. Bucka, P. Heide, G. Ruprecht, and B. Unrau, Phys. Rev. C **55**, 1517 (1997).
[7] G. Ruprecht, D. Bemmerer, K. Czerski, P. Heide, and M. Hoeft, Nucl. Phys. **A688**, 512c (2001).
[8] F. S. Levin, in *Reaction Dynamics* (Gordon and Breach, New York, 1973), p. 20.
[9] J. Yan, F. E. Cecil, J. A. McNeil, M. A. Hofstee, and P. D. Kunz, Phys. Rev. C **55**, 1890 (1997).
[10] M. Hoeft, K. Czerski, P. Heide, and M. Lang, Nucl. Phys. **A688**, 524c (2001).
[11] A. G. Sitenko, *Theory of Nuclear Reactions* (World Scientific, Singapore, 1990).
[12] *Handbook of Mathematical Functions*, edited by M. Abramowitz and I. A. Stegun, NBS Applied Mathematics series 55 (Dover, New York, 1966).
[13] J. M. Blatt and L. C. Biedenharn, Rev. Mod. Phys. **24**, 258 (1952).
[14] G. R. Satchler, *Direct Nuclear Reactions* (Clarendon, Oxford, 1983).
[15] P. D. Kunz, Code DWUCK4, http://spot.colorado.edu/~kunz
[16] P. D. Kunz and E. Rost, in *Computational Nuclear Physics*, edited by K. Langanke, S. E. Koonin, and J. Maruhn, Vol. 2 (Springer, Heidelberg, 1993).
[17] G. Ruprecht, PhD thesis, Tech. Univ. Berlin, (2002), http://edocs.tu-berlin.de/diss/2002/ruprecht_goetz.htm
[18] F. Ajzenberg-Selove, Nucl. Phys. **A490**, 1 (1988).
[19] A. J. Elwyn, R. E. Holland, C. N. Davids, L. Meyer-Schutzmeister, J. E. Monahan, F. P. Mooring, and W. Ray, Jr., Phys. Rev. C **16**, 1744 (1977).
[20] S. Engstler, G. Raimann, C. Angulo, U. Greife, C. Rolfs, U. Schröder, E. Somorjai, B. Kirch, and K. Langanke, Phys. Lett. B **279**, 20 (1992).
[21] S. Engstler, G. Raimann, C. Angulo, U. Greife, C. Rolfs, U. Schröder, E. Somorjai, B. Kirch, and K. Langanke, Z. Phys. A **342**, 471 (1992).
[22] G. R. Satchler, Nucl. Phys. **85**, 273 (1966).
[23] G. Igo, Phys. Rev. **117**, 1079 (1960).
[24] B. A. Watson, P. P. Singh, and R. E. Segel, Phys. Rev. **182**, 977 (1969).
[25] E. Kwaśniewicz and J. Kisiel, Acta Phys. Pol. B **19**, 141 (1988).
[26] C. Spitaleri *et al.*, Phys. Rev. C **63**, 055801 (2001).
[27] A. Musumarra *et al.*, Phys. Rev. C **64**, 068801 (2001).
[28] W. H. Burke, J. R. Risser, and G. C. Phillips, Phys. Rev. **93**, 188 (1954).
[29] C. H. Paris, F. P. G. Valckx, and P. M. Endt, Physica (Amsterdam) **20**, 573 (1954).
[30] J. B. Marion and G. Weber, Phys. Rev. **103**, 1408 (1956).
[31] G. R. Harrison, Gail D. Schmidt, and C. D. Curtis, Phys. Rev. **117**, 532 (1960).
[32] G. Breuer, Z. Phys. **178**, 268 (1964).
[33] D. L. Powell, G. M. Crawley, B. V. N. Rao, and B. A. Robson, Nucl. Phys. **A147**, 65 (1970).

[34] N. Arena, G. Calvi, S. Cavallaro, R. Potenza, and M. Sandoli, Lett. Nuovo Cimento Soc. Ital. Fis. **5**, 879 (1972).
[35] N. Arena, G. Calvi, S. Cavallaro, R. Potenza, and M. Sandoli, Nuovo Cimento Soc. Ital. Fis., A **A38**, 101 (1977).
[36] F. E. Cecil and R. F. Fahlsing, Phys. Rev. C **24**, 1769 (1982).
[37] F. E. Cecil, H. Liu, J. S. Yan, and G. M. Hale, Phys. Rev. C **47**, 1178 (1993).
[38] M. Hoeft, PhD thesis, Tech. Univ. Berlin, 2001.
[39] C. Rolfs and W. S. Rodney, *Cauldrons in the Cosmos* (University of Chicago Press, Chicago, IL, 1988).
[40] C.-P. Wu, F. W. K. Firk, and T. W. Phillips, Phys. Rev. Lett. **20**, 1182 (1968).
[41] H. V. Geramb, K. Amos, R. Sprickmann, K. T. Knöpfle, M. Rogge, D. Ingham, and C. Mayer-Böricke, Phys. Rev. C **12**, 1697 (1975).
[42] S. Cohen and D. Kurath, Nucl. Phys. **A101**, 1 (1967).
[43] C. Prass, diploma thesis, Tech. Univ. Berlin, 1992.
[44] D. N. Spergel *et al.*, Astrophys. J. **148**, 173 (2003).
[45] K. A. Olive, G. Steigman, and T. P. Walker, Phys. Rep. **333**, 389 (2000).